Mat. Res. Soc. Symp. Proc. Vol. 675 © 2001 Materials Research Society

FIELD EMISSION SITE DENSITIES OF NANOSTRUCTURED CARBON

J B Cui, J Robertson, W I Milne,
Department of Engineering, Cambridge University, Cambridge CB2 1PZ, UK

ABSTRACT

The field emission properties of nanostructured carbon films deposited by cathodic vacuum arc in a He atmosphere have been studied by measuring the emission currents and the emission site density. The films have an onset field of ~3 V/μm. The emission site density is viewed on a phosphor anode and it increases rapidly with applied field. It is assumed that the emission occurs from surface regions with a range of field enhancement factors but with a constant work function. The field enhancement factor is found to have an exponential distribution.

INTRODUCTION

Electron field emission from various carbon films, such as chemical vapour deposited (CVD) diamond, CVD graphite, carbon nanotubes, amorphous carbon and nanostructured carbon is of great interest because it occurs from flat films without the need to form microtips [1-19]. Emission from these materials can occur for applied fields of 10 volts per micrometer or less. The emission is however discontinuous, and occurs as the series of spots [20]. The emission site density is therefore an important parameter, particularly for displays. This paper describes field emission properties of nanostructured carbon films deposited at room temperature by cathodic arc. The emission I-V curve and the emission site density were both measured. The discontinuous nature of the emission indicates that emission occurs preferentially from different parts of the surface. We have found that the work function for these carbon films is quite large and varies from 4.5 to 5.0 eV. We propose that the preferential emission therefore arises from a variation in the local field enhancement factor. The emission can be described by a distribution of field enhancement factors.

EXPERIMENT

The nanostructured carbon films were deposited at room temperature using a cathodic vacuum arc system. The base pressure of the deposition chamber was about $5x10^{-7}$ mbar and the deposition pressure could be varied from $1x10^{-6}$ to 1 mbar by introducing helium gas into the chamber. The He thermalises the carbon ions and atoms and allows them to form fullerene-like clusters [21], which are incorporated in the growing film. The thickness of the carbon film is between 10 and 100 nm. The films are deposited onto conductive Si substrates on which there is a 1.5 μm thick resistive ballast layer of photoresist. The function of the ballast layer is to limit the emission current from individual emission spots, and to allow the range of the emission sites to be seen, without saturating the phosphor screen [22]. Ballast resistors are frequently used in Spindt tip field emission devices to even out the current distribution and to prevent excessive currents [23].

The emission is measured in a parallel plate configuration. The anode-to-sample spacing was 50 or 100 μm by using PTFE spacers. An ITO (indium-tin-oxide) or phosphor coated glass is used as an anode to collect the emitted current. The emission spots are displayed on the anode and recorded by a CCD camera while the

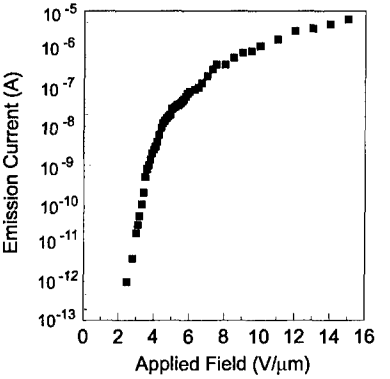

Fig. 1. Field emission I-V curve of carbon film on Si wafer with a ballast layer. Inset is the corresponding Fowler-Nordheim plot.

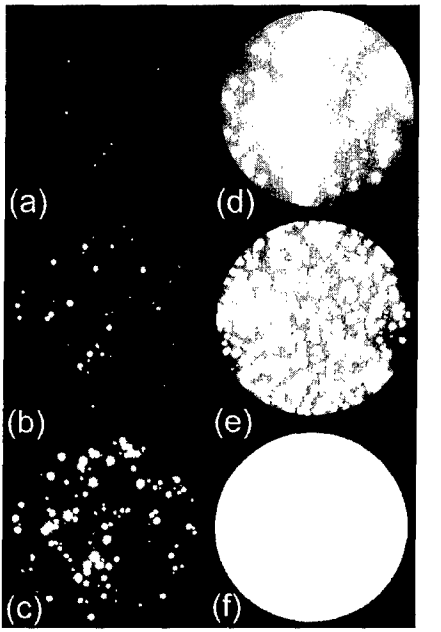

Fig. 2. Field emission images at different applied fields: (a) 4, (b), 6, (c) 8, (d) 11, (e)15, and (f) 20 V/μm.

emission I-V curve is measured. The pressure in the measurement chamber is maintained at 10^{-7} mbar during measurements by a turbo-molecular pump. It should be emphasised that no conditioning process was used for the field emission measurement, unlike is often needed for DLC films [15], because the emission of the nanostructured carbon samples is stable and repeatable.

RESULTS AND DISCUSSION

Fig 1 shows the measured emission current as a function of applied field. The detection limit of our system is ~1 pA. The current rises rapidly above 3 V/μm. The current then rises more slowly above 1 μA due to the effect of the ballast layer. The current limiting causes a downward curvature in a Fowler-Nordheim plot.

Fig. 2 shows the emission image recorded on a CCD camera at increasing applied fields. The emission site density (ESD) was counted at each field after digitisation, and this is plotted against applied field in Fig. 3.

The emission current density J (A/m^2) is expected to obey the Fowler and Nordheim law

$$J = A \cdot \frac{(\beta F)^2}{\phi} \cdot \exp\left(-\frac{B\phi^{3/2}}{\beta F}\right) \qquad (1)$$

F is the applied electric field in V/m, β is the field enhancement factor and ϕ is the potential barrier for the emission surface in eV. A and B are constants equal to 1.56×10^{-2} and 6.83×10^{9}, respectively. To a first approximation, $\beta = h/r$, where h is the height of the emission tip and r the radius of curvature of the tip.

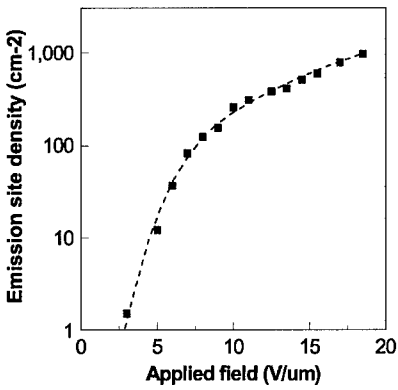

Fig. 3 Field emission site density as a function of applied field. The solid line is a fit for eq (2).

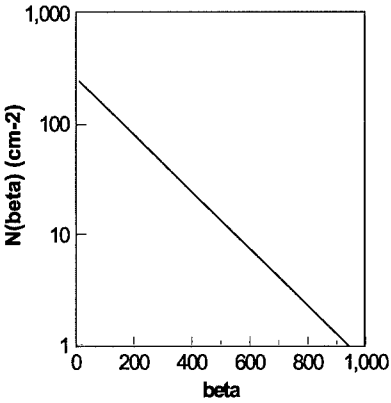

Fig. 4. Emission site density versus field enhancement factor β. The solid line is the fit by eq.(4).

The variation of emission site density with applied field F in Fig. 3 can be fitted by the probability distribution

$$N(F) = N_0 \exp(-\frac{b}{F}) \tag{2}$$

b is a constant. This function is the curve plotted in Fig. 3.

In principle, the ESD could depend on many factors. However, the functional form of eq (2) suggests a simple model. The emission depends on two parameters in (1), the barrier height ϕ and the field enhancement factor β. There has been considerable effort to identify the value of the emission barrier in carbon systems, in part to answer the fundamental question of why emission occurs at relatively low fields [23]. In the case of diamond, the fully hydrogenated surface has a negative electron affinity and the work function can be lower than 3.5 eV [25,26]. Diamond-like carbons are found to have work functions of 4.3 to 5 eV, and they are less sensitive to the surface termination than is diamond [14]. Nanotubes also have a work function of order 5 eV [8]. The work function of the films in this study was measured by Kelvin probe and it lies in the range 4.7±0.1 eV [27].

We therefore approximate that the *local* barrier ϕ is constant, and attribute the discontinuous emission to a variation in the local field enhancement factors at the sites. Following Groning et al [8], if an emission site becomes visible at a certain value of current, then (1) implies

$$F_{loc} = \beta F = \text{const} \tag{3}$$

Thus, the distribution (2) can be expressed as an exponential distribution of β values

$$N(\beta) = N_0 \cdot \exp(-\frac{\beta}{\beta_0}) \tag{4}$$

where β_0 is a constant. This distribution is plotted in Fig. 4.

Groning et al [8] used a similar analysis to describe the ESD in carbon nanotube films. In carbon nanotubes, if we assume that the tubes have a similar radius and length, then the β distribution arises from the effect of inter-tube screening. The presence of nearby nanotubes screens the electric field intensification at a tube tip [9], unless the tube separation d is about over twice the tube height h, d>2h. This is not true in typical nanotube mats, and this accounts for the observed β distribution. It is likely that a similar effect occurs in nanostructured carbon. The entire surface has a similar work function. There may be many regions with a large β. The screening effect of one on the other and fractal effects in the surface curvature are likely to lead to a Poisson distribution of β values as seen here.

The total emission current, I, can be estimated by adding the current from all sites. If we assume that once on, a site emits a current given by eq (1), then

$$I = \int J(\beta).S.N(\beta).d\beta = \int_0^{\beta_{max}} J \cdot S \cdot \exp(-\frac{\beta}{\beta_0})d\beta \qquad (5)$$

where the β_{max} is the maximum β that is observed experimentally, S is the emission area of one site. An effect of the distribution of β's is that while each emission site will obey the Fowler-Nordheim (FN) equation, the total emission current from (5) does not. The FN plots for each emission site is a straight line with a slope of $6.83 \times 10^9 \phi^{1.5}/\beta$. The effect of the β distribution is to produce a slight upward curvature of the FN plots. This contrasts with the downward curvature at high currents caused by current limiting by the ballast layer.

A more detailed analysis of FN plots with a β distribution was given by Levine [28]. He described the case of emission from Spindt tips, and assumed a gaussian distribution of a 'tip bluntness' parameter B in the reduced FN equation

$$J = A.\exp(-\frac{B}{V}) \qquad (6)$$

with

$$N(B) = N_0 \exp(-\frac{(B-B_0)^2}{2\sigma^2}) \qquad (7)$$

The advantage of a gaussian distribution is that the integral (5) is now analytic. Qualitatively, β is proportional to 1/B, so our exponential distribution corresponds to the lower wing of the gaussian distribution of B.

This work was supported by EPSRC. We thank K Teo for the site counting software and Samsung for the phosphor plates.

REFERENCES

1. N.S. Xu, R.V. Latham, Y.Tzeng, Electron. Lett.**29**, 1596 (1993).
2. A. A. Talin, L. S. Pan, K. F. McCarty, T. E. Felter, Appl. Phys. Lett. **69**, 3842(1996).

3. F Lacher, C Wild, D Behr, P Koidl, Diamond Related Mats **6** 1111 (1997)
4. D.Zhou, A.R. Krauss, D.M. Gruen, J.Appl.Phys. **83**, 4546(1997).
5. W. Zhu, G.P. Kochanski, S. Jin, Science **282**, 1471 (1998).
6. K. A. Dean and B. R. Chalamala, Appl. Phys. Lett. **76**, 375(1999).
7. W Zhu, C Bower, O Zhou, G Kochanski, S Jin, App Phys Lett **75** 873 (1999)
8. O Groning, O M Kuttel, C Emmenegger, P Groning, L Schlapbach, J Vac Sci Technol B **18** 665 (2000).
9. L Nilsson, O Groning, C Emmenegger, O Kuttel, E Schaller, L Schlapbach, H Kind, J M Bonard, K Kern, App Phys Lett **76** 2071 (2000)
10. V I Merkulov, D H Lowdnes, L R Baylor, J App Phys 89 1933 (2001)
11. J M Bonard, N Weiss, H Kind, T Stockli, L Forro, K Kern, A Chatelain, Advanced Mats 13 184 (2000)
12. J M Bonard, H Kind, T Stockli, L O Nillson, Solid State Electronics (2001)
13. B. F. Coll, J.E. Jaskie, J.L. Markham, E.P.Menu, A.A. Talin, and P. von Allmen, Mater. Res. Soc. Symp. Proc. **498**, 185 (1998).
14. V I Merkulov, D H Lowndes, L R Baylor, App Phys Lett **75** 1228 (1999)
15. B S Satyanarayana, J Robertson, W I Milne, J App Phys **87** 3126 (2000)
16. A Ilie, A Hart, A J Flewitt, J. Robertson, W I Milne, J App Phys **88** 6002 (2000)
17. A N Obratztsov, I Y Pavlovsky, A P Volkov, J Vac Sci Technol B **17** 674 (1999)
18. B.S. Satyanaryana, A. Hart, W.I. Milne, and J. Robertson, Appl. Phys. Lett. **71**, 1430 (1997).
19. A Hart, B.S. Satyanarayana, W. I. Milne, and J. Robertson, Appl. Phys. Lett. **74**, 1594 (1999).
20. A A Talin, in 'Amorphous Carbon, State of Art', ed S R P Silva et al, (World Scientific, Singapore, 1998)
21. P Milani, S Iannotta, 'Cluster beam synthesis of nano-structured materials', (Springer, Berlin, 1999)
22. J.B. Cui, J. Robertson, and W.I. Milne, J App Phys **89** 3490 (2001).
23. A Ghis, R Meyer, P Raumbaud, F Levy, T Leroux, IEEE Trans ED **38** 2520 (1991)
24. J Robertson, J Vac Sci Technol B 17 659 (1999), Mat Res Soc Symp Proc **621** xxx (2000)
25. J. B. Cui, J. Ristein, M. Stammler, K. Janischwosky, G. Kleber, and L. Ley, Diamond Rel. Mater. 9, 1143 (2000)
26. R.Schlesser, M.T. McClure, W.B. Choi, J.J.Hren, and Z. Sitar, Appl. Phys. Lett. **70**, 1596(1997).
27. A Ilie, A. C Ferrari, T Yagi, J. Robertson, J App Phys (Aug 1, 2001)
28. J. D. Levine, J. Vac. Sci. Technol. **B 13** 553 (1994).